Presented: ENC, Orlando, March 99

System theoretic aspects of NMR spectroscopy

Raimund J. Ober
Cancer Immunobiology Center
UT Southwestern Medical Center at Dallas
Dallas, TX 75235-8576, USA

Permanent address: Center for Engineering Mathematics
University of Texas at Dallas
Richardson, TX 75083, USA
Email: raimund@skylab.swmed.edu

E. Sally Ward
Center for Immunology and Cancer Immunobiology Center
6000 Harry Hines Boulevard
UT Southwestern Medical Center at Dallas
Dallas, TX 75235-8576, USA
Email: sally@skylab.swmed.edu

1 Introduction

System theory (see e.g. [2]) has played a major role over the past decades in many fields such as engineering. Powerful techniques which have been developed in system theory have been applied successfully to a large array of problems. Here we show how NMR spectroscopy can also be described in the language of system theory. System theoretic methods are used to address a number of problems in NMR spectroscopy. We discuss results that describe characterizations of possible NMR spectra given a fixed quantum mechanical system. In addition, we discuss the processing of NMR data and in particular new parameter estimation methods.

2 Master System

2.1 Schrödinger equation, restricted to spin dynamics

$$\dot{\psi} = -i(H_1 + \sum_{j=1}^{2} H_{2,j} u_j(t))\psi$$

where

- H_1 is Hamiltonian corresponding to strong magnetic field.
- $H_{2,j}$ is Hamiltonians corresponding to time-varying magnetic field (inputs).
- H_1, H_2 hermitian.
- u_1, u_2 inputs, i.e. the excitation pulses.

2.2 Density matrix description (Master system)

$$\dot{\sigma}(t) = -i[H_1, \sigma(t)] - i\sum_{j=1}^{k} u_j(t)[H_{2,j}, \sigma(t)] - \hat{R}[\sigma(t) - \sigma_{eq}],$$

$$y(t) = trace(M\sigma(t)), \quad t \geq t_0,$$

- y measured output (induced magnetization).
- $\hat{R}$ relaxation superoperator.
- M measurement operator.
- σ_{eq} equilibrium density matrix.

3 Bilinear system

Set

- $c(t) = vec(\sigma(t)) - vec(\sigma_{eq}), \quad t \geq 0.$
- $A = -i(I \otimes H_1 - H_1^T \otimes I) - R.$
- $N_j := -i(I \otimes H_{2,j} - H_{2,j}^T \otimes I), \quad j = 1, 2.$
- $b_j := N_j vec(\sigma_{eq}), \quad j = 1, 2.$
- $c = (vec(M^T))^T.$

Under mild assumptions the master system is equivalent to the bilinear system ([7])

$$\dot{c}(t) = Ac(t) + (\sum_{j=1}^{2} u_j(t)N_j)c(t) + \sum_{j=1}^{2} b_j u_j(t),$$

$$y(t) = cc(t).$$

- Bilinear systems are extensively studied in systems and control theory (see e.g. [9]).

4 One-Dimensional Experiments

- Spectrum ([7])

$$Real(c(i\omega - A)^{-1}c_0),$$

where c_0 is the state of the system at the time when detection starts.

5 Two-Dimensional Experiments

- 2-dimensional time signal

$$s(t_1, t_2), \quad t_1 \geq 0, t_2 \geq 0$$

- 2-dimensional Fourier transform is (special case) ([7])

$$G(\omega_1, \omega_2) = c(i\omega_1 I - A)^{-1} T_3 (i\omega_2 I - A)^{-1} c_0$$

where

- c_0 is the state at the end of the preparation period.
- T_3 is a matrix 'associated' with the mixing period.

6 Classification of 1-D experiments

Addition schemes (e.g. phase cycling):

- Several different (single scan) experiments are run.
- The resulting measurements (fids) are added.

Theorem 6.1 *([8]) The set of all one-dimensional spectra obtainable using addition schemes is given by*

$$\{c(i\omega - A)^{-1}c_0 \mid c_0 \in \mathcal{E}\},$$

where $\mathcal{E}$ is the smallest subspace of $\mathbb{C}^n$ that

1. contains b_1 and b_2

2. and is invariant under A, N_1 and N_2.

7 Classification of 2-D experiments

Addition schemes (e.g. phase cycling):

- Several different (single scan) experiments are run.
- The resulting measurements (fids) are added.
- Resulting spectrum

$$G(\omega_1, \omega_2) = c(i\omega_1 I - A)^{-1} \left(\sum_{j=1}^{k_2} \lambda_j T_{3,j} \right) (i\omega_2 I - A)^{-1} \left(\sum_{l=1}^{k_1} \mu_j c_{1,l} \right).$$

Theorem 7.1 *([8]) The set of all two-dimensional spectra obtainable using addition schemes is given by*

$$\{c(i\omega_1 - A)^{-1} T_3 (i\omega_2 I - A)^{-1} c_0 \mid T_3 \in \mathcal{T}, c_0 \in \mathcal{E}\},$$

where

1. $\mathcal{E}$ is the smallest subspace of $\mathbb{C}^n$ that

(a) contains b_1 and b_2

(b) and is invariant under A, N_1 and N_2.

2. $\mathcal{T}$ is the matrix algebra generated by A, N_1 and N_2.

If addition schemes are not permitted, then the characterization of all obtainable spectra becomes more difficult. The questions are most naturally posed using notions such as the set of reachable states of the underlying bilinear systems ([4]).

8 From data to spectral parameters

Find a state space realization, i.e. (A_k, b_k, c_k) s.t.:

$$fid(n\Delta T) \approx c_k A_k^{n-1} b_k, \quad n = 1, 2, \ldots,$$

where ΔT is the sampling interval (see e.g. [3],[1],[6]).

Diagonalize A_k, i.e.

$$T A_k T^{-1} =: diag(\alpha_1, \ldots, \alpha_k) =: dA_k,$$

Then with $dB_k := Tb_k$, $dC_k := C_k T^{-1}$,

$$fid(n) \approx dC_k dA_k^{n-1} dB_k = \sum_{j=1}^{k} \gamma_j \beta_j \alpha_j^{n-1}, \quad n = 1, 2, \ldots,$$

where $dB_k = (\beta_1 \cdots \beta_k)^T$, $dC_k = (\gamma_1, \cdots, \gamma_k)$.

As

$$\alpha_j \approx e^{(2\pi i\omega_j - d_j)\Delta T}, \quad j = 1, 2, \ldots, k,$$

the **frequency estimates** are

$$\hat{\omega}_j = \frac{angle(\alpha_j)}{2\pi\Delta T}, \quad j = 1, 2, \ldots, k,$$

the estimates of the **damping factors** are

$$\hat{d}_j = \frac{-log|\alpha_j|}{\Delta T}, \quad j = 1, 2, \ldots, k.$$

For two-dimensional data a similar approach can be carried out using realization algorithms for two-dimensional systems ([5]).

9 Data processing

Algorithms were tested that are based on the above formulation of NMR experiments using simulated data of a COSY type spectrum of a coupled two spin system (Figure 1 and 2). The simulations were carried out first with noise free data and then with noisy data (Figures 1-12). To test how well the proposed methods can extend short data sets the original noise free data set was reduced to the subset of its first 16 by 16 data points. Figures 3 and 4 show the spectrum that is obtained after zero-filling this data set. The multiplet structure of the spectrum is no longer resolved. This 16 by 16 data set was then extended to a 1024 by 1024 data set. The spectrum (Figures 5 and 6) was compared with the spectrum of the actual full data set. The errors between the extended data and the actual data was less than 10^{-8} which indicates that for practical purposes the extensions provide perfect reconstructions of the actual data in the noise free case. The estimates of the spectral parameters were also essentially perfect up to machine precision.

The proposed methods are also designed to be able to deal with noisy data. To test this property a relatively high level of white noise was added to the simulated data (see Figure 7). Due to the high level of noise the extensions and parameter estimates for the 16 by 16 data set were no longer reliable. However, for a 128 by 128 data set almost perfect noise suppression and data extension to the full data length could be achieved (Figure 8). For a 32 by 32 data subset very good noise suppression and somewhat acceptable data reconstruction could be achieved (Figures 11 and 12). For the same 32 by 32 data set zero-filling provided unacceptable spectral resolution (Figures 9 and 10). The parameter estimates for the 128 by 128 data set produced very good parameter estimates with errors of less than one percent (and significantly better depending on the precise implementation of the approach). As can be inferred from Figure 12 the accuracy of the parameter estimates for the 32 by 32 data set was less good but still acceptable considering the noise level.

References

[1] H. Barkhuijsen, R. De Beer, and D. Van Ormondt. Improved algorithm for noniterative time-domain model fitting to exponentially damped magnetic resonance signals. *Journal of Magnetic Resonance*, 73:553–557, 1987.

[2] T. Kailath. *Linear Systems*. Prentice Hall, 1980.

[3] S. Kung. A new identification and model reduction algorithm via singular value decomposition. In *Proceedings 12th Asilomar Conference on Circuits, Systems and Computers, Pacific Grove, CA, IEEE*, pages 705–714, 1978.

[4] R. J. Ober, V. Ramakrishna, and E. S. Ward. On the role of reachability and observability in NMR experimentation. Report Center for Engineering Mathematics, University of Texas at Dallas, July 1998.

[5] R. J. Ober and E. S. Ward. Genuine two-dimensional processing of two-dimensional NMR data. to be submitted.

[6] R. J. Ober and E. S. Ward. Correcting for phase distortion of NMR spectra analyzed using singular value decomposition of Hankel matrices. *Journal of Magnetic Resonance Series A*, 114:120–123, 1995.

[7] R. J. Ober and E. S. Ward. System theoretic formulation of NMR experiments. *Journal of Mathematical Chemistry*, 20:47–65, 1996.

[8] R. J. Ober and E. S. Ward. On the class of attainable multidimensional NMR spectra. *Journal of Mathematical Chemistry*, 22:1–10, 1997.

[9] W. J. Rugh. *Nonlinear System Theory*. The Johns Hopkins University Press, 1981.

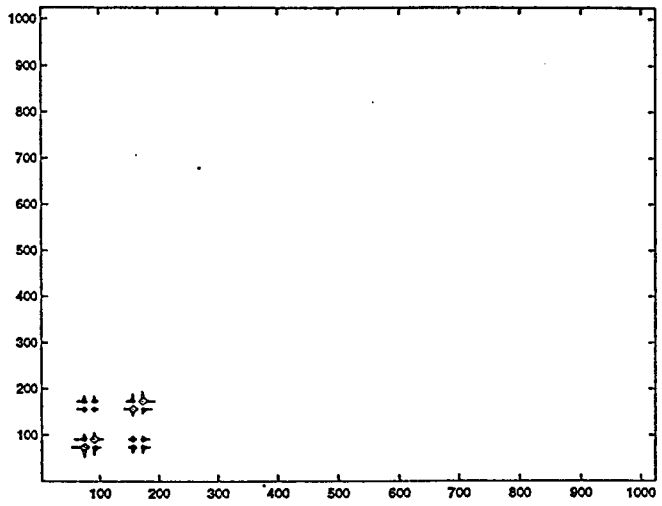

Figure 1:
Two dimensional spectrum of simulated noise free 1024 x 1024 data set (in absolute value mode).

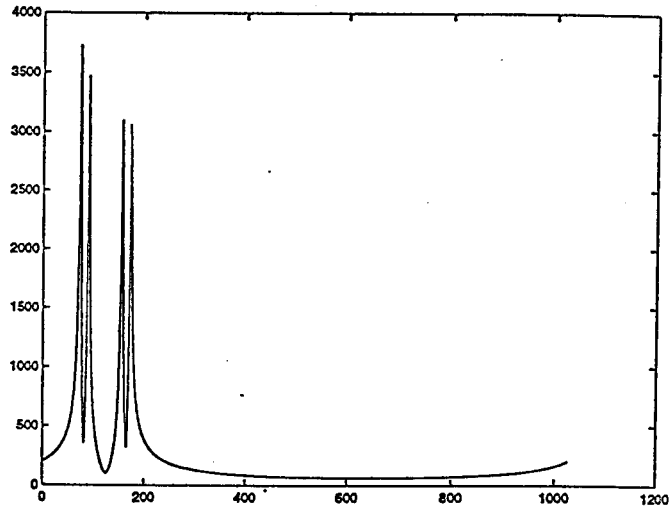

Figure 2:
One-dimensional slice of spectrum in Figure 1.

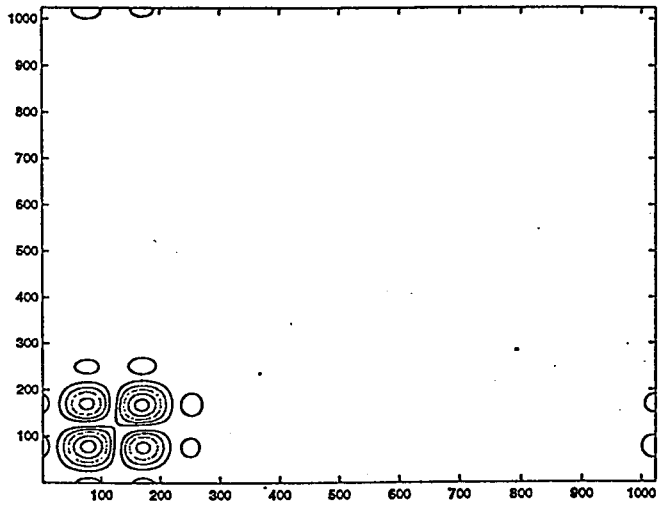

Figure 3:
Of the data set of Figure 1 the 16x16 subset of data points was retained that corresponds to the first 16 points in the t1 and t2 dimensions. This 16x16 dataset was then zero filled and Fourier transformed.

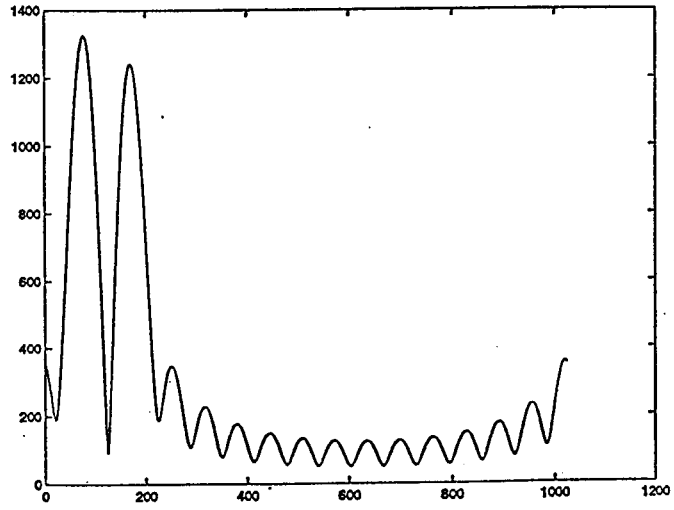

Figure 4:
One-dimensional slice of spectrum in Figure 3. There is a clear loss of resolution in comparison to Figure 2.

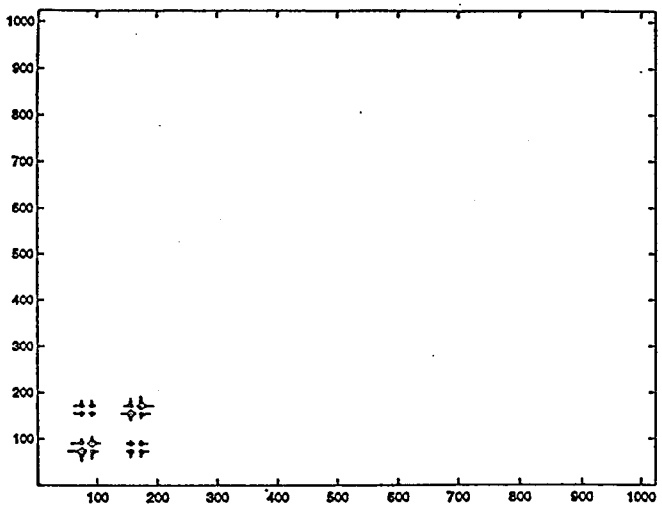

Figure 5:
The same 16x16 subset of the data set as in Figure 3 was extended to a 1024x1024 data set using Method 1 as described in the proposal. The resulting extended data set was then Fourier transformed. A numerical comparison between this spectrum and the spectrum of the full data set in Figure 1 shows indicates that the spectra are essentially identical up to round off errors.

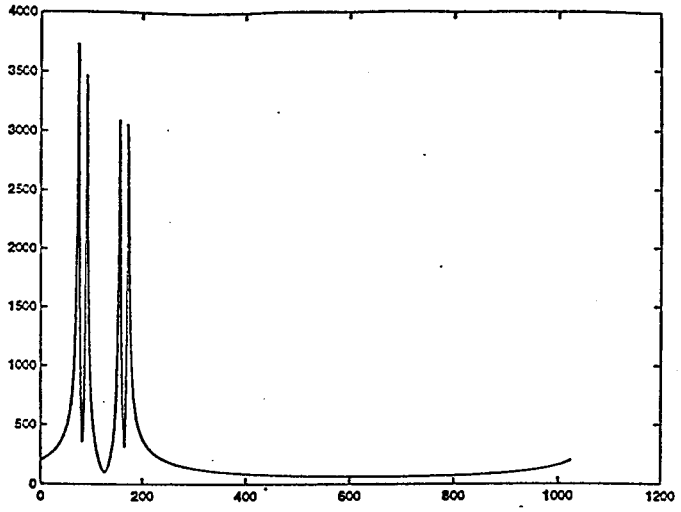

Figure 6:
One dimensional slice of spectrum in Figure 5. It demonstrates that the proposed method has recovered the resolution of the original simulated data in stark contrast to zero filling as can be seen in comparison with Figure 4.

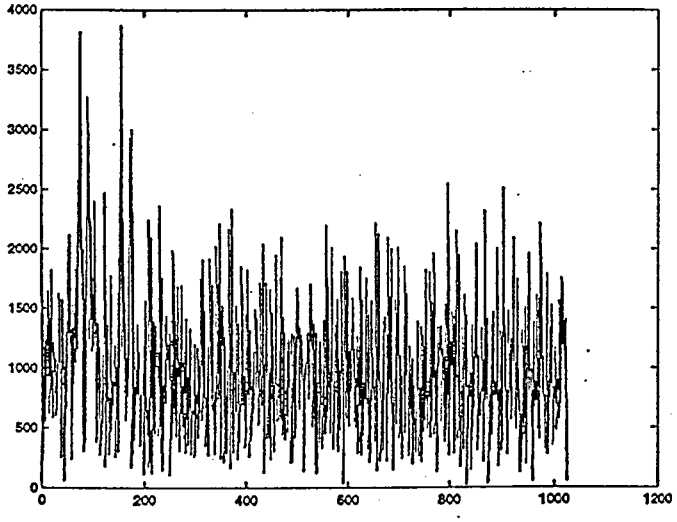

Figure 7:
One dimensional slice of the spectrum of the same data as in Figures 1 and 2, but with white noise added to the time domain data.

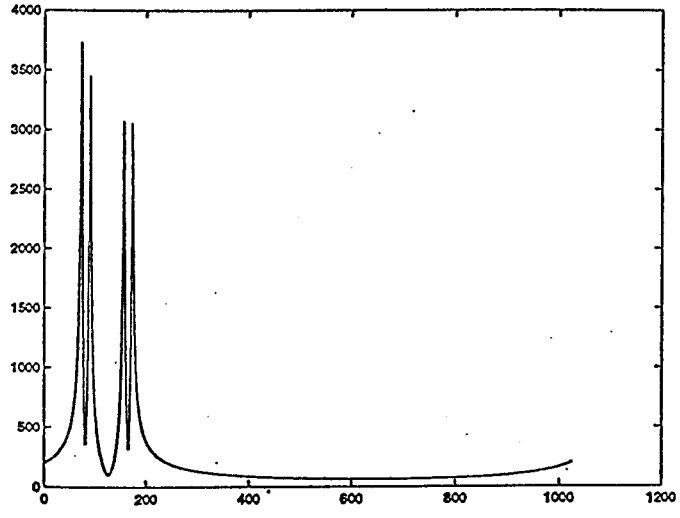

Figure 8:
The noisy data set of Figure 7 has been reduced to a 128x128 data set. This figure shows the same slice of the spectrum as in Figures 2 and 7 after processing with Method 1. There is essentially no difference to the noise free and full data case of Figure 2.

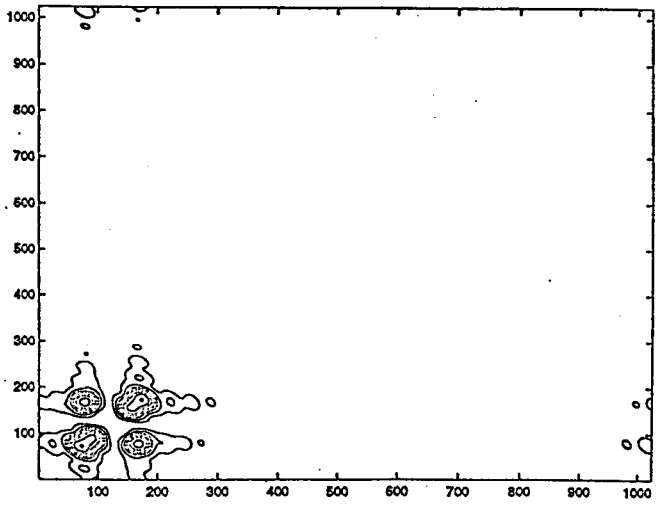

Figure 9:
A 32x32 subset of the noisy data set of Figure 7 was zero filled. The resulting spectrum does not resolve the multiplet structure.

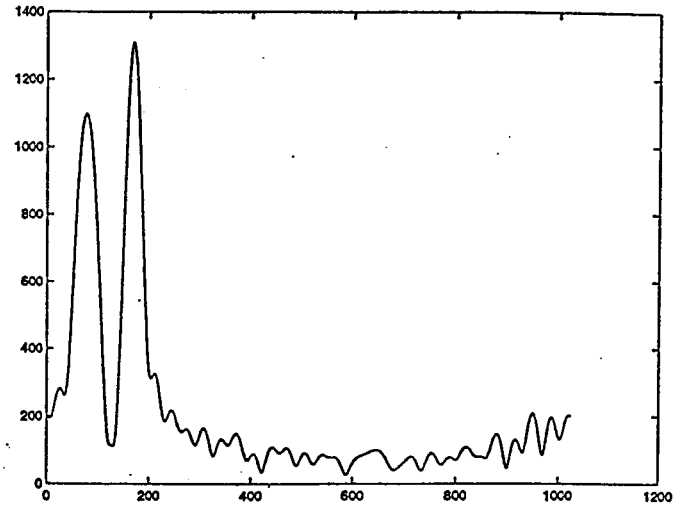

Figure 10:
One dimensional slice of spectrum of Figure 9.

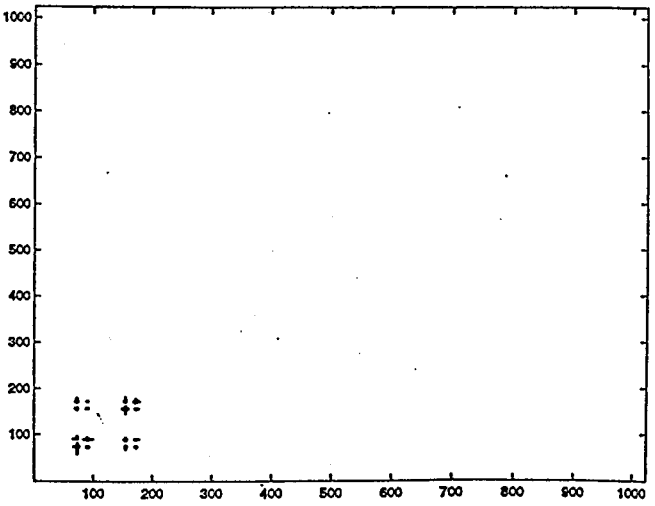

Figure 11:
Two dimensional spectrum after noisy 32 by 32 data set has been noise reduced and extended using Method 1. In contrast to zero filling (Figure 9) the multiplet structure is fully resolved.

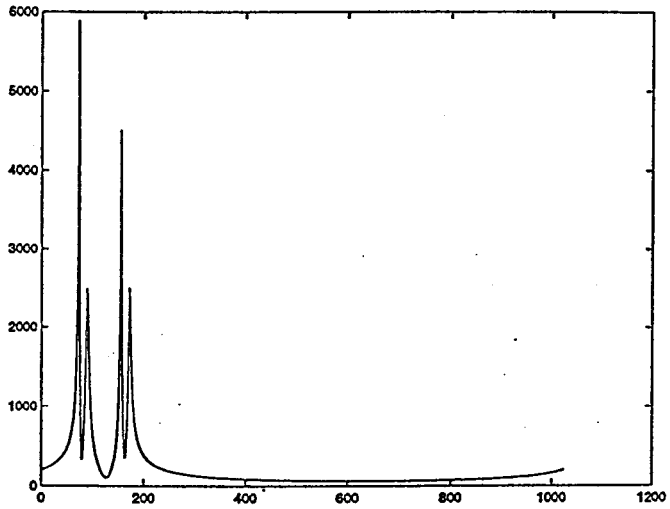

Figure 12:
One dimensional slice of spectrum in Figure 11. Clearly the noise reduction was successful. However, in contrast to the noise free case of Figure 6 and the case of the larger noisy data set of Figure 8 some perturbations of the spectrum are introduced. Nevertheless, unlike processing solely based on zero-filling (Figure 10) the method could recover the essential features of the spectrum.